Developing Steam Bubble Cavitation for Pollutant Degradation: Determining Hydroxyl Radical Production Under Selective Conditions

Emily Marron
Undergraduate Honors Thesis
Department of Civil and Environmental Engineering
May 14th, 2012

Under the supervision of:

Dr. Linda Weavers
Professor of Civil and Environmental Engineering
The Ohio State University
470 Hitchcock Hall
2070 Neil Avenue
Columbus, OH 43210

and

Dr. Meiqiang Cai
Associate Professor
College of Environmental Science and Engineering
Zhejiang Gongshang University
Jiaogong Road 149
Hangzhou 310035, P. R. China

ABSTRACT

Current wastewater treatment processes in the U.S. are not designed to remove pharmaceuticals and personal care products (PPCPs). Effects of long term, low exposure of PPCPs on humans and ecosystems are largely unknown, resulting in a growing concern over exposure to these pollutants. Advanced oxidation processes (AOPs) using highly reactive hydroxyl radicals (•OH) are promising technologies to remove these contaminants. •OH reacts with inorganic and organic compounds in water to produce less harmful products. The formation and collapse of microbubbles to generate •OH is the advanced oxidation technique known as cavitation. The energy efficiency of current cavitation techniques, such as acoustic and hydrodynamic cavitation, is limiting their use in environmental engineering. A recent study proposed steam cavitation as a considerably more energy efficient cavitation process. Steam cavitation is the method of injecting steam into sub-cooled water to produce cavitation. Because only one study has been conducted on this process, this research project aimed to further investigate the use of steam cavitation to efficiently generate •OH. The objectives of this research were: (1) to design a reactor to successfully create steam cavitation, and (2) to vary temperatures and nozzle diameters in steam cavitation to determine optimum parameters for the greatest •OH generation. After iterative experimentation and calculation, a temperature-constant reactor was constructed to produce steam cavitation. Steam was injected through a nozzle into the pool-water reactor containing terephthalate. Generated •OH from the bubble collapse reacted with terephthalate to form hydroxyterephthalate. Therefore, concentrations of hydroxyterephthalate corresponded to •OH formation. Results indicate that •OH production is dependent on the pool-water temperature and the nozzle diameter. Of the conditions tested, 45°C

and a nozzle diameter of 0.61 mm produced the most •OH. Therefore, steam cavitation produces •OH, warranting further study of this process as a novel water treatment technology.

INTRODUCTION

Overview

Pharmaceuticals and personal care products (PPCPs) have been detected in numerous surface and ground waters across the U.S. The impacts of these emerging contaminants on both humans and ecological systems are not fully understood. Current drinking water and wastewater treatment processes are not designed to remove these compounds (1, 2). To address this issue, alternative treatment methods are being investigated as a means of removing PPCPs from water. In particular, advanced oxidation processes (AOPs) have been shown to be an effective technique in degrading contaminants such as PPCPs (3, 4). AOPs are expensive technologies, but are sometimes necessary to remove toxic compounds resistant to treatment by other technologies. AOPs are grouped together because they form highly reactive and strongly oxidizing hydroxyl radicals (•OH). These radicals react with organic and inorganic compounds present in water to produce typically less harmful products, thus reducing the toxicity of the water. Conventional AOPs include using a combination of oxidizing agents (such as O_3 and H_2O_2) or exposure to ultraviolet light (4).

More recent technologies in advanced oxidation include the use of cavitation, which is the formation, growth, and subsequent violent collapse of microbubbles formed in a liquid. Under conditions of high temperature (>5000 K) and pressure (>1000 atm) created by the collapse of the microbubble, the following reaction occurs:

$$H_2O \longrightarrow H\bullet + \bullet OH \qquad [1]$$

The temperature within the bubble at the end of collapse dictates the amount of •OH formed. The temperature achieved is a complicated function of the bubble size, the pool water temperature, the amount of water vapor in the bubble, and the bubble temperature at the start of collapse (5). Cavitation is a result of many different phenomena. Traditional cavitation techniques include

hydrodynamic and acoustic cavitation. Hydrodynamic cavitation occurs from pressure variations in flowing liquid, which is caused by a change in geometry of the system (6). Acoustic cavitation occurs as a result of ultrasonic waves as microbubbles collapse from wave-forced compression and refraction. Although ultrasonic cavitation has been shown to be effective in reducing toxicity of water, the treatment is energy intensive, limiting its practicality (4).

In a recent study, Mahulkar et al. proposed an innovative technique using steam bubbles to generate cavitation (7). In steam bubble cavitation, steam is directly injected into sub-cooled water using a nozzle, resulting in the production of steam microbubbles that collapse as the pressure of the vapor in the bubble falls below the vapor pressure. Figure 1 shows a conceptual diagram of the steam bubble collapse.

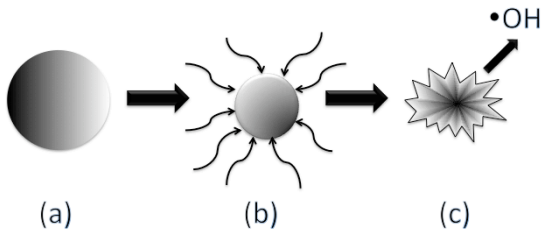

Figure 1: Steam bubble collapse. From (a) to (b), the steam bubble is immersed into subcooled water, where condensation of steam occurs due to the temperature difference. As the bubble wall implodes (c), inertial forces compress the remaining gas inside the bubble, resulting in heating of the gaseous water; this heating causes the subsequent formation of •OH.

The initial size of the steam bubble may be altered by the steam flux (calculated from the nozzle diameter and steam flow) through the nozzle and the pool temperature (8). Mahulkar et al. showed that steam bubble cavitation oxidized iodide; and they estimated, based on calculations, that the process would be nearly 10 times more energy efficient when coupled with acoustic cavitation than conventional acoustic cavitation alone (7).

This study aimed to look further into the process of steam bubble cavitation. The technique of steam bubble cavitation is very attractive as a cavitation process due to its energy

efficiency. Because there has only been one preliminary study of this novel process, there is much room for further investigation. Particularly, this study aimed to design and build an improved experimental set-up compared to the initial report. Using the improved design, both nozzle diameter and pool temperature were varied to work towards determining optimal experimental conditions to generate the greatest concentration of hydroxyl radicals, which are key to the degradation of toxic compounds. The initial hypothesis was that ideal collapse conditions would be created with lower pool temperatures and smaller nozzle diameters, since smaller bubbles surrounded by more extreme temperatures would have a more violent collapse and a high end-collapse temperature. Initial results do not completely agree with this hypothesis; however, further testing is required to establish trends between •OH formation and experimental conditions. Future work should be performed to optimize steam bubble cavitation while demonstrating its efficiency in both •OH formation and energy use. These efficiencies together may make the technique advantageous as a novel water treatment technology.

Objectives

The purposes of this study were to: (1) design a reactor to successfully create steam bubble cavitation and (2) vary temperatures and nozzle diameters in the steam cavitation process in order to determine the best parameters for the greatest generation of hydroxyl radicals (•OH). Further investigating conditions forming •OH by steam bubble cavitation is the stepping point to scale the process up to be used as a water treatment technology. This study was part of a larger project within the research group of Dr. Linda Weavers of Ohio State and visiting professor Dr. Meqiang Cai of Zhejiang Gongshang University to better understand steam bubble cavitation and collapse conditions for •OH formation.

MATERIALS AND METHODS

Experimental Set-up

Figure 2 shows a schematic of the steam bubble cavitation experimental set-up. First, a steam-generating device (Figure 3) was designed and constructed by modifying a commercially available stainless steel pressure cooker (Fagor Duo Pressure Cooker). The pressure cooker was placed on a heat source (a 1300-Watt Waring Pro Single Burner). The lid of the pressure cooker was fitted with three ports: (1) an outlet with a control valve for excess steam release (used for pressure control), (2) an outlet with a control valve leading to the needle tip which was inserted into the reactor, and (3) a temperature/pressure gage. The needle was attached to the steam-generating device using a luer-lock fitting (Hamilton Metal Hub Needles).

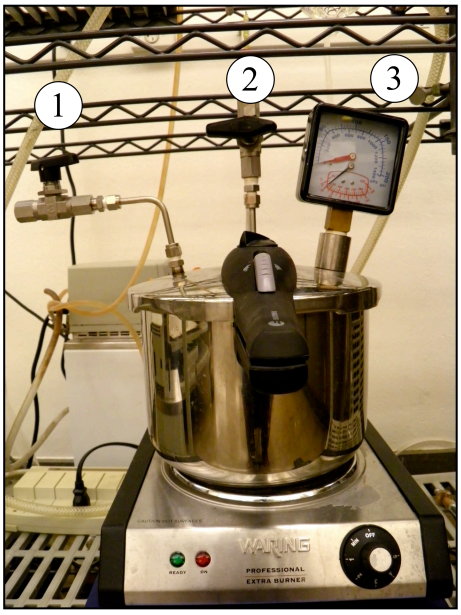

Figure 3: Pressure cooker with (1) control valve, (2) valve leading to steam release into reactor, and (3) temperature/pressure gauge

The generated steam traveled through tubing to a needle acting as a nozzle. From the nozzle, the steam traveled into the pool-water reaction solution. The pool-water reaction solution was water-jacketed.

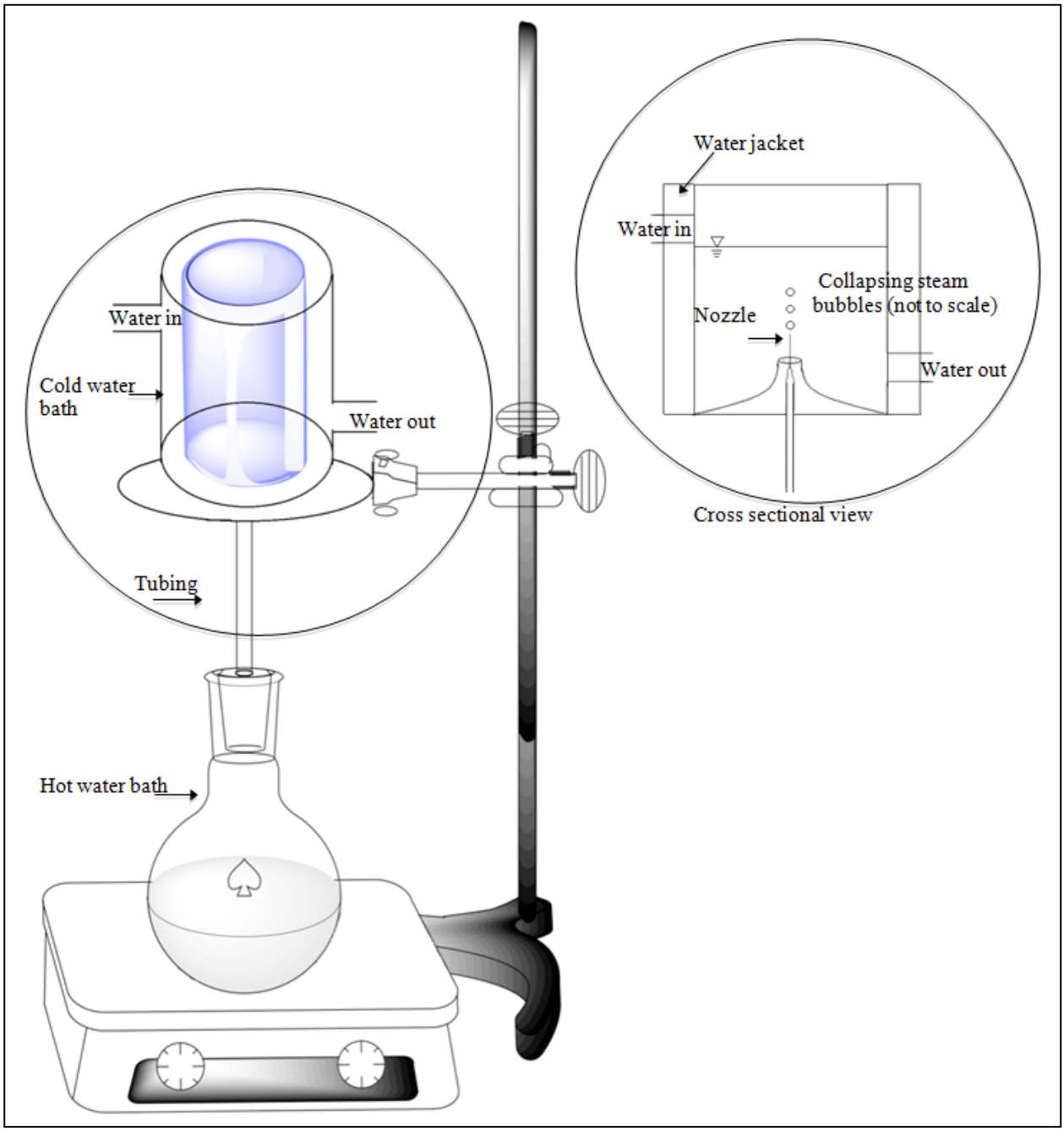

Figure 2: Schematic of steam bubble cavitation with major components identified.

Experimental Methods

For each experiment, the pressure cooker was filled with deionized water. The water was heated to a boiling temperature of about 115°C and pressurized to a gauge pressure between 75 and 100 kPa. While the water heated, the cooling water baths ran until each reached a constant

temperature. The valve providing steam flow into the reactor was opened completely to allow for maximum steam flow. For all experiments, the outlet valve was closed to keep an adequate pressure inside the steam-generating pressure cooker. Steam flow through the needle varied with the needle diameter. Experimental parameters tested are shown in Table 1.

Table 1: Parameters adjusted in steam bubble cavitation during experimentation

Nozzle Inner Diameters (mm)		
0.61	0.84	
Water Bath Temperatures (°C)		
20	30	45

To detect •OH formation from steam bubble cavitation, buffered 2 mM terephthalate (TA) was used as the pool-water reaction solution based on Mason et al. (9). The trapping of hydroxyl radicals with TA has been shown to be a sensitive and useful technique in quantifying •OH generated (10). The reaction of •OH with TA is shown below:

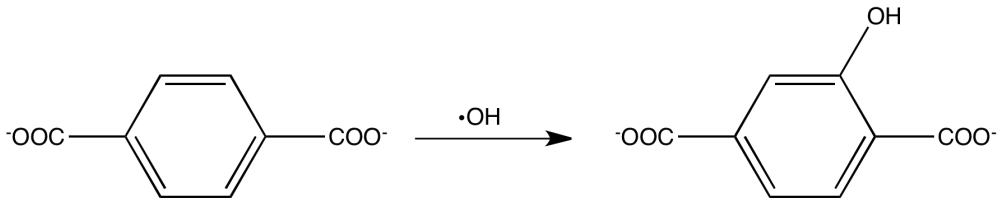

[2]

The product of this reaction, hydroxyterephthalate (HTA), is fluorescent.

Analytical Methods

Fluorescence measurements of the HTA concentration in each of the samples was determined using a Shimadzu RF-5301PC spectrofluorometer with parameters including a beam slit width of 1.5 nm, excitation wavelength of 315 nm, and emission wavelength of 425 nm (11). To quantify the concentration of HTA formed in each sample, a calibration curve (Figure 4) was constructed from a 2 mM buffered HTA stock solution.

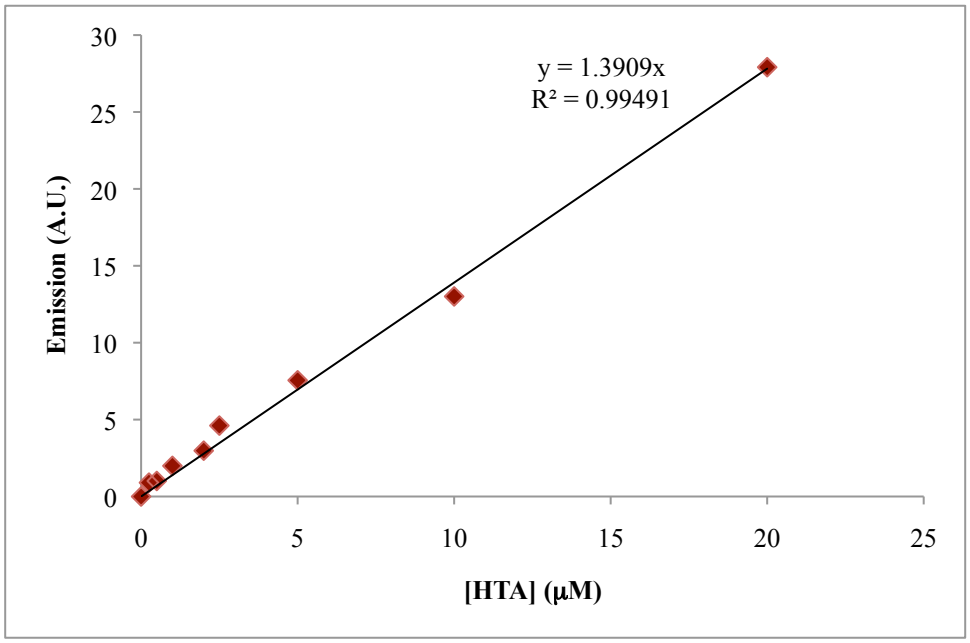

Figure 4: HTA calibration curve created by taking emission readings at a range of concentrations. Dilutions were performed using a buffered stock solution of 2mM HTA (4-25-2012)

RESULTS AND DISCUSSION

Designing the Experimental Set-up and Heat Transfer Calculations

Figure 5 below shows the first reactor design. The first reactor held a volume of about 25 mL. The maximum reaction time in the initial reactor was about 5 minutes. After 5 minutes, the reactor overflowed due to added volume from condensed steam (with an average steam flow of 3 mL/min and starting TA volume of 10 mL). In this initial design for a steam bubble cavitation reactor, several factors were not considered.

Initial experiments revealed three main problems with the initial reactor design. The first problem was temperature control. The condensed steam added significant heat to the reactor solution. In monitoring the reactor temperature, the solution heated up to nearly 60°C in one minute, and continued to increase throughout the duration of the experiment. Secondly, the HTA concentration in the reaction solution was below the limits of detection for the spectrofluorometer. It was decided that a longer reaction time was necessary to ensure detection of •OH formation from steam bubble cavitation. Lastly, with the longer reaction time, a larger increase in volume from steam condensation would occur. In order to keep a constant temperature, give ample time for the production of •OH, and provide sufficient volume, a new reactor was designed.

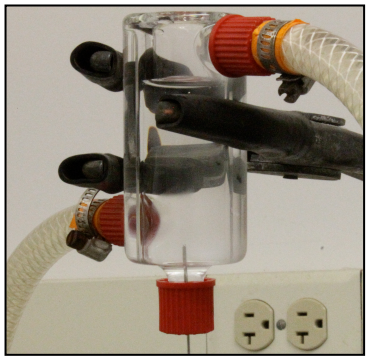

Figure 5: Initial steam bubble cavitation reactor

To provide adequate temperature control in the new reactor, heat transfer calculations were performed to estimate the cooling area required to compensate for added energy from the steam. To maximize the amount of cooling surface area within the reactor, a cooling coil was chosen rather than the water jacket used in the initial reactor. Preliminary testing supported this design; a cooling coil immersed into the reactor solution proved to be a more effective cooling component than the water jacket. A standard glass coil size, to be used within a cylindrical reactor, was chosen. The glass coil had the following dimensions: inner tubing diameter of 0.005 m, outer tubing diameter of 0.007 m, outer coil diameter of 0.028 m. Figure 6 illustrates the coil structure. Once the total cooling surface area required was calculated, the number of cycles of the specified cooling coil was, in turn, calculated.

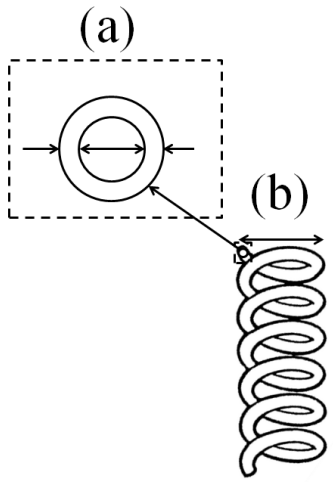

Figure 6: Figure of cooling coil, where (a) illustrates the inner (0.005 m) and outer (0.007 m) diameter of the cooling tube and (b) illustrates the outer diameter (0.028 m) of the cooling coil.

To calculate the cooling area required, energy from heat input into the system (Q), heat transfer coefficient of the system (K), and temperature difference between the reactor solution and cooling water bath (ΔT) were determined:

$$A = \frac{Q}{K\Delta T} \qquad [3]$$

In calculating the total cooling area (A), a ΔT of 40°C (or 40 K) was assumed based on a pool-water solution temperature of 52.5°C and a cooling coil temperature of 12.5°C. Next, energy from heat input into the system (Q) was calculated:

$$Q = F\left[\Delta H_1 + \Delta H_2(T_{steam} - 100) + \Delta H_3(100 - T_{water})\right] \quad [4]$$

where F is the steam flow rate of 15 mL/min (0.015 kg/min), ΔH_1 is the potential enthalpy of water vapor (2257.2 kJ/kg), ΔH_2 is the enthalpy of steam (0.2163 kJ/kg-K), and ΔH_3 is the enthalpy of water (0.4326 kJ/kg-K). Using these values with a maximum steam temperature (T_{steam}) of 119°C and solution temperature of 52.5°C (T_{water}), Q was calculated to be 34.37 kJ/min, or 572.83 Watts.

Finally, the heat transfer coefficient, K, was calculated using coefficients from three different resistive components of the process: the heat transfer coefficient from the cooling coil in water (λ_1), the heat transfer coefficient of glass (λ_2), and the convective coefficient of the reactor solution (λ_3). The first value, the coefficient for the cooling coil (λ_1), was calculated using Equation 5,

$$\lambda_1 = \frac{\mathrm{Nu} \times 0.618}{d} \quad [5]$$

where Nu is the Nusselt number and d is the inner diameter of the cooling tube. The Nusselt number is a dimensionless value that describes the convection heat transfer occurring at the surface (12). The value of the Nusselt number (Equation 6) is dependent on both the Reynolds number and the Prandtl number. The n in Equation 6 was 0.4 due to the fact that the pool-water solution was heated.

$$\mathrm{Nu} = 0.023\mathrm{Re}^{0.8}\,\mathrm{Pr}^{n} \quad [6]$$

Thus, before calculating the Nusselt number, the Reynolds number and Prandtl number were calculated in Equations 7 and 8. The Reynolds number, which characterizes the flow of a liquid,

was calculated for the flow of water through the cooling tube. The Reynolds number is dependent on the liquid flow rate (Q) through the tube, the hydraulic diameter of the tubing (D_h), the kinematic viscosity of water (ν), and the cross-sectional area (A) of the tubing. Using all of these parameters, the Reynolds number was calculated to be 5412.

$$\mathrm{Re} = \frac{QD_h}{\nu A} = \frac{2.778 \times 10^{-5} \ \frac{\mathrm{m}^3}{\mathrm{s}} \times 0.005 \ \mathrm{m}}{1.307 \times 10^{-6} \frac{\mathrm{m}^2}{\mathrm{s}} \times \left(\frac{\pi}{4} 0.005^2 \ \mathrm{m}^2 \right)} = 5412 \qquad [7]$$

The Prandtl number is the ratio of kinematic viscosity to thermal diffusivity. In other words, the Prandtl number describes the relative effectiveness of both momentum and energy transport via diffusion in the momentum and thermal boundary layers (12). In Equation 8, the Prandtl number is calculated from the specific heat of water (C_p), the dynamic viscosity of water (μ), and the thermal conductivity of water (k).

$$\mathrm{Pr} = \frac{C_p \mu}{k} = \frac{\left(4.174 \times 10^3 \frac{\mathrm{J}}{\mathrm{kg} \cdot \mathrm{K}} \right) \left(0.001307 \frac{\mathrm{Ns}}{\mathrm{m}^2} \right)}{0.618 \ \frac{\mathrm{W}}{\mathrm{m} \cdot \mathrm{K}}} = 8.83 \qquad [8]$$

Plugging Reynolds and Prandtl numbers into Equation 6, the Nusselt number was calculated to be 53.30. Finally, λ_1 was calculated using the Nusselt number in Equation 5:

$\lambda_1 = \frac{\mathrm{Nu} \times 0.618}{d} = \frac{53.30 \times 0.618 \frac{\mathrm{W}}{\mathrm{m} \cdot \mathrm{K}}}{0.005 \ \mathrm{m}} = 6588 \frac{\mathrm{W}}{\mathrm{m}^2 \cdot \mathrm{K}}$. Again, this was the heat transfer coefficient of the cooling coil. Two correction factors were applied to this coefficient. The first was used (Equation 8) to correct for elbows in the coil, which would affect the flow through the tubing. The second (Equation 9) was to correct for the transition between laminar and turbulent flow during previous calculations.

$$h' = \left(1 + 1.77\frac{d}{r}\right)h = \left(1 + 1.77\frac{0.005}{0.012}\right)h = 1.74h \quad [8]$$

In Equation 8, *d* is the inner diameter of the cooling tube (0.005 m) and *r* is the radius of the cooling coil (0.012 m), as shown in Figure 7.

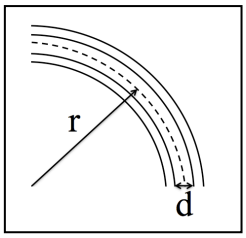

Figure 7: Illustration of parameters for the elbow correction factor in Equation 8, where *d* is the inner diameter of the cooling tube and *r* is the radius of the coil.

$$h' = \left(1 - \frac{6\times10^4}{\mathrm{Re}^{1.8}}\right)h = \left(1 - \frac{6\times10^4}{5412^{1.8}}\right)h = 0.989h \quad [9]$$

Multiplying the original λ_1 by the correction factors in Equations 8 and 9 gives a new value, λ_1':

$$\lambda_1' = (1.74)\times(0.989)\times\left(6588\frac{\mathrm{W}}{\mathrm{m}^2\cdot\mathrm{K}}\right) = 11{,}316\frac{\mathrm{W}}{\mathrm{m}^2\cdot\mathrm{K}} \quad [10]$$

The second component of the overall heat transfer coefficient was to account for the heat transfer through glass, the reactor material. Equation 11 divides the heat transfer coefficient of glass by the thickness of the glass tubing (0.002 m) to get a value of 3100 W/m^2-K.

$$\lambda_2 = \frac{\lambda_{glass}}{d} = \frac{6.2\frac{\mathrm{W}}{\mathrm{m}\cdot\mathrm{K}}}{0.002\ \mathrm{m}} = 3100\frac{\mathrm{W}}{\mathrm{m}^2\cdot\mathrm{K}} \quad [11]$$

The third and last component of the overall heat transfer coefficient represents the fact that the liquid within the reactor is not actively mixed, i.e. the flow of the reactor solution is stagnant. λ_3 is the convective heat transfer coefficient of the reactor liquid–a standard value of 220 W/m^2-K.

$$\lambda_3 = 220\frac{\mathrm{W}}{\mathrm{m}^2\cdot\mathrm{K}} \quad [12]$$

Combining λ_1, λ_2, and λ_3 in Equation 13 yields an overall heat transfer coefficient, *K*, of 202 W/m^2-K.

$$\frac{1}{K} = \frac{1}{\lambda_1'} + \frac{1}{\lambda_2} + \frac{1}{\lambda_3} = \frac{1}{11316} + \frac{1}{3100} + \frac{1}{220} = 0.00496 \frac{\text{m}^2 \cdot \text{K}}{\text{W}} \quad [13]$$

$$K = 202 \frac{\text{W}}{\text{m}^2 \cdot \text{K}} \quad [14]$$

Using results for *Q* (from Equation 4), *K* (from Equation 14), and ΔT (40 K), the cooling area (*A*) was calculated by plugging the values back into Equation 3 (shown in Equation 15). The final cooling area required was calculated to be 0.071 m^2.

$$A = \frac{Q}{K\Delta T} = \frac{34.37 \ \frac{\text{kJ}}{\text{min}} \times \frac{1 \text{ min}}{60 \text{ s}} \times \frac{1000 \text{ J}}{1 \text{ kJ}}}{202 \frac{\text{W}}{\text{m}^2 \cdot \text{K}} \times (40 \text{ K})} = 0.071 \text{ m}^2 \quad [15]$$

The standard coil size previously described and shown in Figure 6 was used for the remainder of the calculations. To determine the total length of the tubing required from the calculated surface area, the equation for the surface area of a cylinder was used ($A=\pi dL$). Additionally, a factor of $\ln(d_2/d_1)$ was included, where d_2 and d_1 are the outer and inner diameters of the tubing, respectively. The factor took the thickness of the tubing into account. Equation 16 shows the total length (*L*) of cooling tube required, 1.52 m.

$$A = \frac{\pi dL}{\ln\left(\frac{d_2}{d_1}\right)} \Rightarrow L = \frac{A \cdot \ln\left(\frac{d_2}{d_1}\right)}{\pi d} = \frac{0.071 \text{ m}^2 \cdot \ln\left(\frac{0.007 \text{ m}}{0.005 \text{ m}}\right)}{\pi(0.005 \text{ m})} = 1.52 \text{ m} \quad [16]$$

To determine how many circles, or cycles, could be created with 1.52 m of cooling tubing and a specified coil circumference, Equation 17 was used.

$$L = \text{circumference} \times n \text{ cycles} = \pi d \times n \quad [17]$$

Plugging in values to Equation 17 yielded 18 cycles, using the previously specified coil diameter of 0.028 m, or 28 mm.

$$n = \frac{L}{\pi d} = \frac{1.52 \text{ m}}{\pi \cdot 0.028 \text{ m}} = 17.28 = 18 \text{ cycles} \quad [18]$$

Once the total cooling surface area and the number of cycles required were calculated, the last part of the design was to calculate the total volume required for maximum steam flow and sufficient reaction time. For a flow of 15 mL/min and a reaction time of 60 minutes, the volume required was 900 mL, as shown in Equation 19. A reaction time of 60 minutes was assumed to provide ample time for •OH formation.

$$\text{Volume needed} = 15 \frac{\text{mL}}{\text{min}} \times 60 \text{ min} = 900 \text{ mL} = 9 \times 10^{-4} \text{ m}^3 \quad [19]$$

Using 900 mL and a diameter of 0.035 m, the height of the reactor was calculated (Equation 20).

$$V = \frac{\pi}{4} d^2 h \Rightarrow h = \frac{4V}{\pi d^2} = \frac{4\left(9 \times 10^{-4} \text{ m}^3\right)}{\pi\left(0.035 \text{ m}\right)^2} = 0.935 \text{ m} \quad [20]$$

An additional 600 mL was added to the 900 mL to get a total volume of 1500 mL. The addition was meant to compensate for the volume loss due to the immersed cooling coil, and also to provide adequate volume for a steam flux greater than 15 mL/min.

From calculations for the cycles of cooling coil, it was decided that the entire reactor did not require cooling. The reactor was designed to be about 1 m tall, with the bottom half (50 cm) fitted with cooling components. Due to the large size, 60 cycles of cooling coil were added along with an outer water jacket for extra cooling capacity to further ensure a constant reaction temperature. The inner diameter of the top 50 cm was about 5.5 cm, and the inner diameter of the bottom 50 cm was a bout 3.5 cm (with a water jacket). The total volume of the new reactor is

about 1535 mL. Figure 8 shows a rough sketch of the reactor with dimensions and labels. Figure 9 shows a photo of the new, redesigned reactor. Parts are also labeled and described in Figure 9.

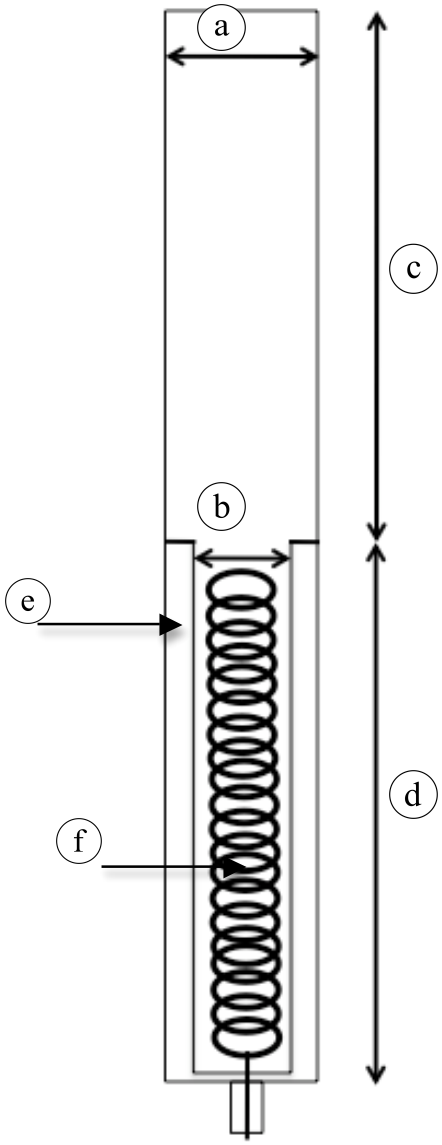

Figure 8: Sketch of new, redesigned reactor with corresponding major dimensions. The upper diameter (a) is 5.5 cm, lower diameter (b) is 3.5 cm, and the top and bottom halves, (c) & (d) are each 50 cm. The two cooling components on the bottom half of the reactor, water jacket (e) and cooling coil (f), are also pictured.

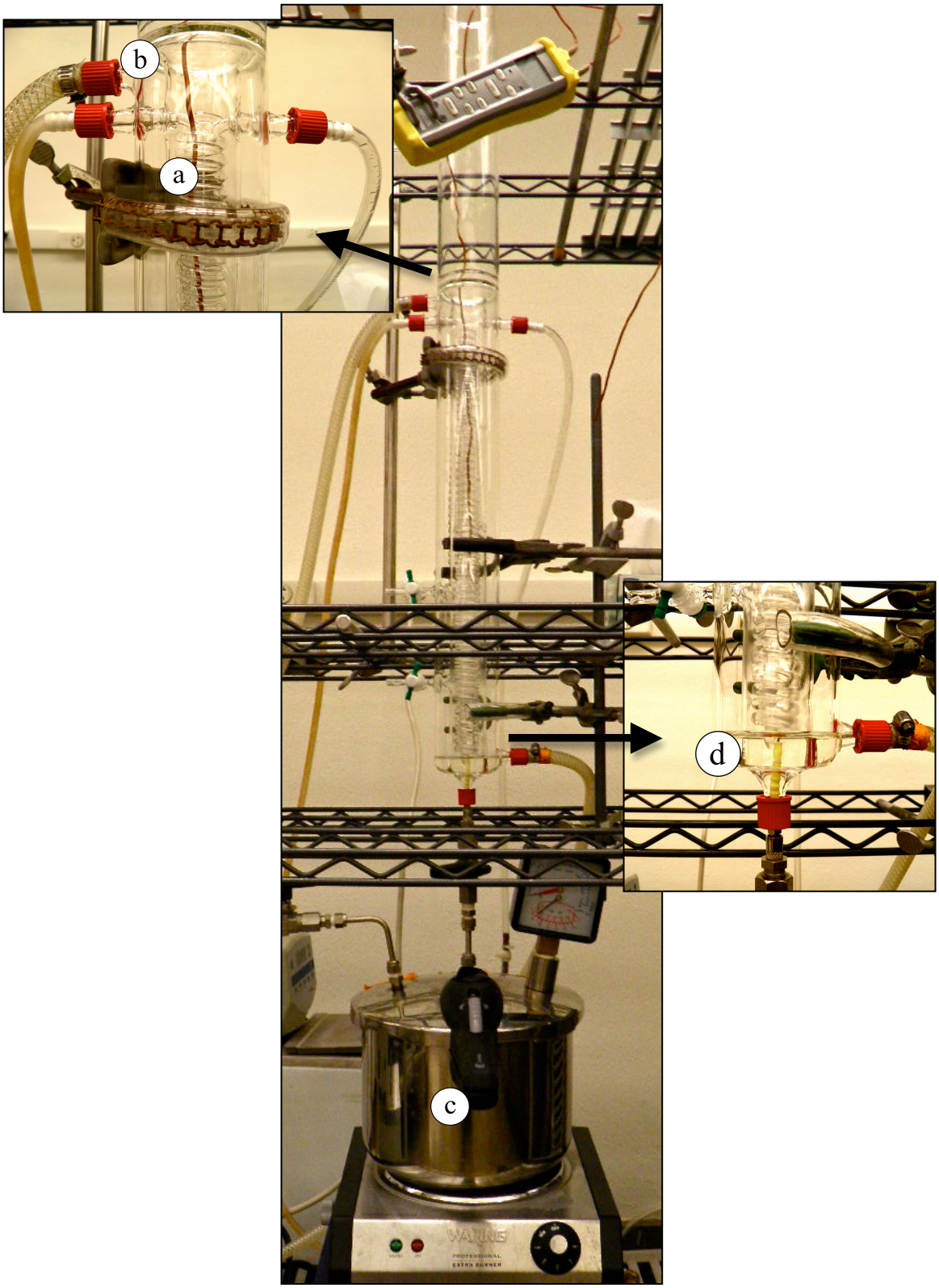

Figure 9: Improved steam bubble cavitation reactor outfitted with (a) inner cooling coil, (b) outer cooling jacket, (c) steam generating device, (d) needle immersed in reactor.

Verifying Reactor Design

After the new reactor was constructed, its ability to perform as designed was tested. The reactor was tested for its ability to maintain a constant temperature. The water jacket and inner coil were each connected to a separate water bath (Fisher Scientific Isotemp 1016S and Thermo NESLAB RTE7) set to 10 and 5°C, respectively. Steam at a flow rate of about 10 mL/min was introduced into the reactor for 50 minutes. Several runs were completed, and the temperature of the pool-water solution only increased 3 or 4 degrees. However, as shown in Figure 10, the cooling bath hooked up to the inner coil (cooling bath 1, in blue) increased with the temperature of the pool-water solution within the reactor (reactor solution, in black).

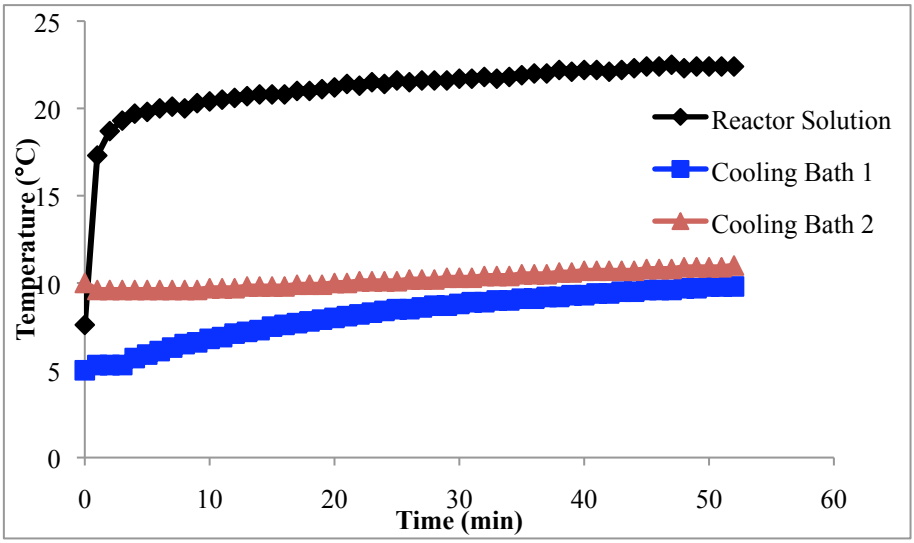

Figure 10: Temperature curves for the reactor solution and cooling baths over 52 minutes (4-5-2012)

Although a change of only a few degrees over 52 minutes is relatively small, reasoning behind the increase in temperature was investigated. In examining the experimental set-up during a temperature-monitoring experiment, bubbles were seen forming on the surface of the needle (Figure 11). It was hypothesized that the steam flowing through the needle caused the surface of the needle to heat up, resulting in bubble nucleation on the warm needle surface. Bubbles were an indication of the heat loss in the needle. To prevent the heat loss from occurring, the needle

was insulated with PTFE-silicone septa (Figure 11). An insulated needle was suspected to improve temperature stability in the reactor and provide a more violent bubble collapse, as the steam would maintain a higher temperature before entering the pool-water solution.

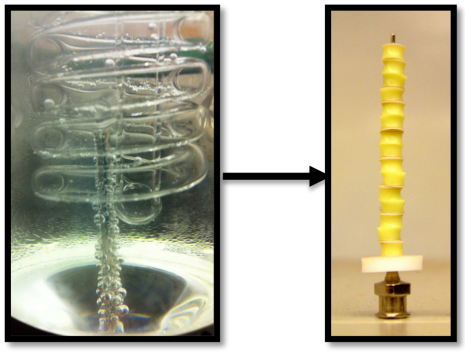

Figure 11: On the left, bubbles forming on warm needle surface. On the right, insulated needle to prevent heat transfer from needle to surrounding solution

Figure 12 shows the temperature monitoring after insulating the needle. The reactor solution (black line) stayed relatively constant (±1°C) for the duration of the 52-minute reaction time. The needle insulation is thought to be the cause of this improvement in temperature control. All experiments conducted with terephthalate post-needle insulation were monitored closely for temperature. For all experiments, the reactor solution maintained a constant temperature as exhibited in Figure 12.

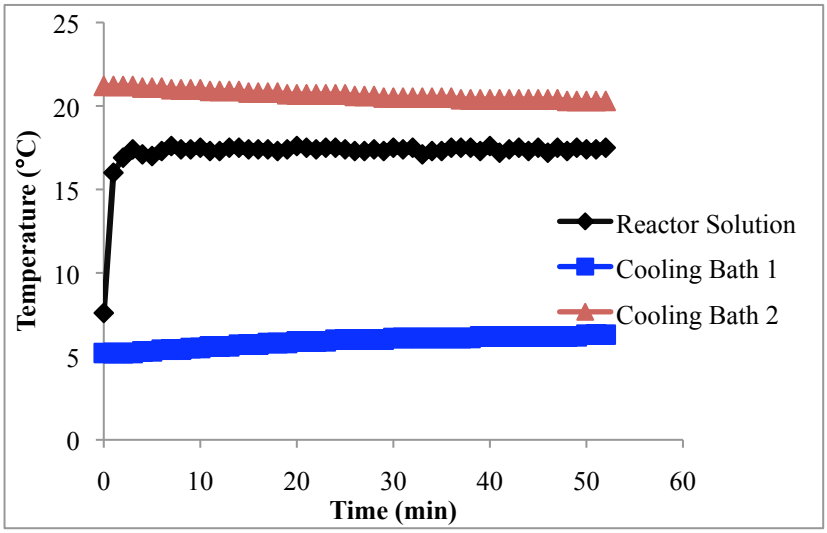

Figure 12: Temperature curves for the reactor solution and cooling baths over 52 minutes after needle insulation (4-23-2012)

Concentration of HTA in new reactor design

In preliminary experiments, HTA was not detected in samples. To detect HTA, samples had to be concentrated. Each experiment with TA ran for 52 minutes. The total amount of solution at the end of the reaction time was dependent on the steam flow, which was dependent on the nozzle diameter used. Upon completion of the experiment, the sample volume was measured and thoroughly mixed. Regardless of the nozzle diameter used, 300 mL of the final mixed sample volume was taken to be concentrated. Samples were concentrated to less than 10 mL each time using a heating plate and stirring rod. The concentrated sample was then tested in the spectrofluorometer for HTA formation. Figure 13 outlines the experimental procedure used for each of the six trials.

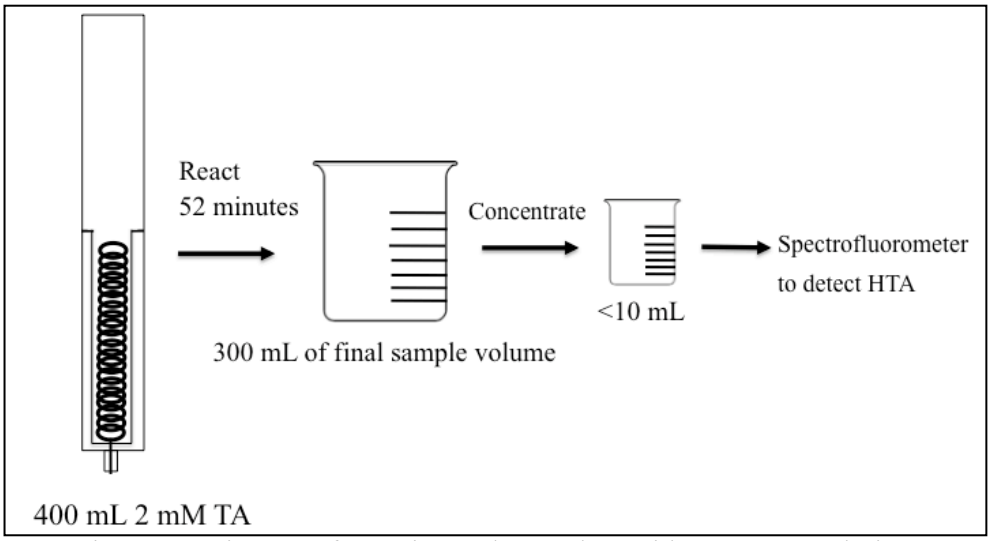

Figure 13: Diagram of experimental procedure with new reactor design

To determine if concentrating the sample caused any loss of HTA through volatilization, a control experiment was conducted. In the experiment, 225 mL of 1μM HTA was concentrated to 20 mL. Fluorescence readings were taken before and after concentration, and it was determined that there was about a 95% recovery of HTA. Therefore, concentrating samples did not result in significant HTA loss and thus did not impact final results.

Hydroxyl Radical Production in new reactor design

As mentioned in the Methodology section, •OH selectively reacted with TA present in the pool-water reactor solution to form HTA, a fluorescent product. Samples that had been concentrated were tested in the spectrofluorometer for HTA. A peak was detected in each of the six concentrated samples, indicating the presence of HTA, and therefore the formation of •OH.

Table 2 summarizes each of the six experiments, providing detailed information about the experimental conditions and subsequent results.

Table 2: Experimental parameters and results from six experiments using two nozzle diameters and three pool-water reactor solution temperatures.

Needle Diameter (mm)	0.84			0.61		
Steam Temperature (°C)	115			115		
Steam Pressure – Gauge Pressure (kPa)	75-100			75-100		
Temperature reactor solution (°C)	21	33	45	17	32	45
Starting Volume (mL)	410	400	400	400	400	400
Final Volume (mL)	777	750	760	545	545	550
Reaction Time (min)	52	52	52	52	52	52
Steam flow (g/min)	7.06	6.73	6.92	2.79	2.79	2.88
Steam flux (kg/m^2-s)	212.26	202.43	208.21	159.02	159.02	164.51
Sample taken to concentrate (mL)	300	300	300	300	300	300
End volume after concentrating (mL)	7.4	5.5	4.4	6	7	7
Concentration factor	40.54	54.55	68.18	50.00	42.86	42.86
Emission (A.U.)	2.1	1.3	2.5	1.3	1.5	3.3
[HTA] in concentrated solution (μM)	1.51	0.93	1.80	0.93	1.08	2.37
[HTA] in experiment sample (μM)	0.0372	0.0171	0.0264	0.0187	0.0252	0.0554
Mass HTA produced (μmoles)	0.0289	0.0129	0.0200	0.0102	0.0137	0.0304
HTA production rate (nmoles/min)	0.556	0.247	0.385	0.196	0.264	0.586
HTA production rate/steam flow	0.0788	0.0424	0.0557	0.0703	0.0946	0.203

Due to the abundance of TA in the pool-water solution, it was assumed that each •OH produced reacted selectively with TA to form HTA. The total mass of HTA produced in each 52-minute experiment was determined by multiplying the concentration of HTA (μM) detected in the 300 mL experiment sample by the final sample volume. The mass of HTA produced over the 52 minutes was converted to a production rate (nmoles/min). Because only one time point was taken, the HTA production rate was assumed to be zero-order, meaning the HTA production

should have increased linearly with time. This assumption is consistent with other work in HTA production rates from •OH formation (11); however, additional experiments should be conducted at several time points between 0 and 52 minutes to verify this assumption. Figure 14 shows the HTA production rates for each of the six conditions tested.

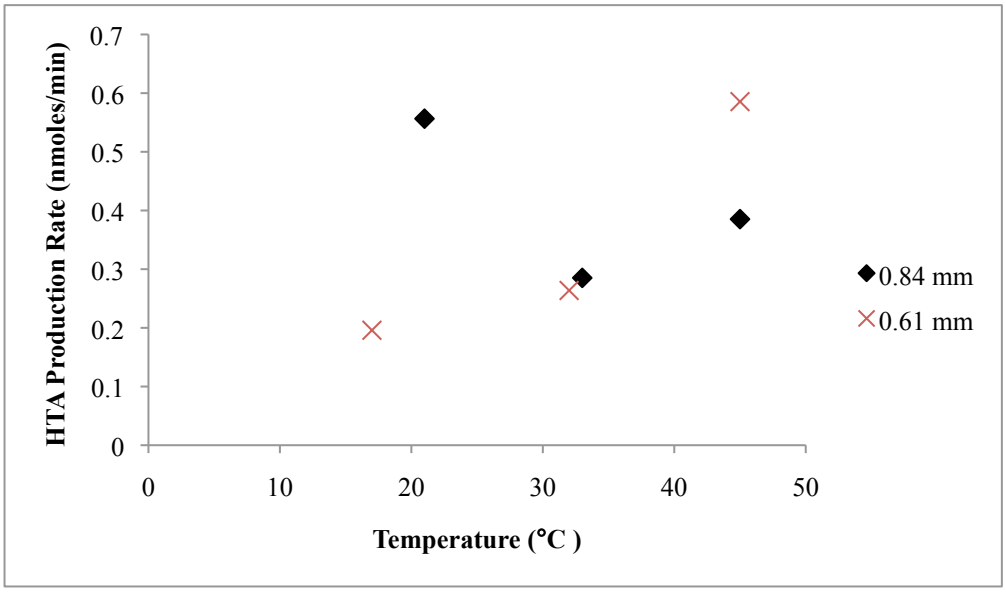

Figure 14: HTA production rate for experiments using nozzle diameters of 0.84 and 0.61 mm at 20, 30, and 45°C (4-25 to 4-30-2012)

Of the six conditions tested, the 0.61 mm nozzle diameter at 45°C had the highest HTA production rate, and therefore produced the most •OH. This result is comparable to the optimum conditions determined by Mahulkar et al.: 0.75 mm nozzle and a pool water temperature of 50°C (7). The optimum condition of this study is even more visible when the steam flow through the nozzle is taken into account along with the HTA production rate. Figure 15 shows the HTA production rate (nmoles/min) per steam flow (g/min) for each of the conditions tested. This was done to normalize the energy input into the system.

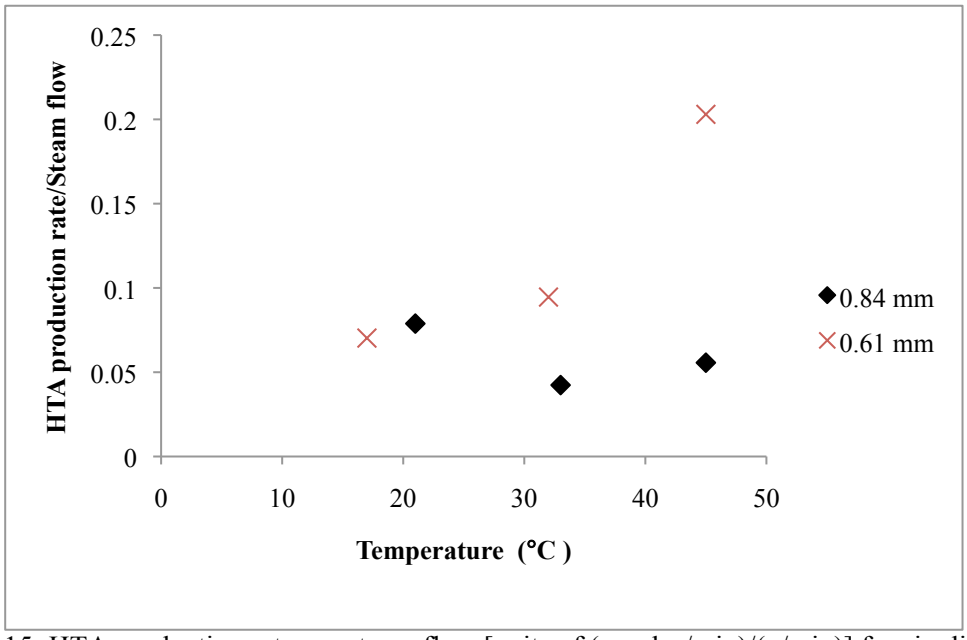

Figure 15: HTA production rate per steam flow [units of (nmoles/min)/(g/min)] for six different conditions (4-25 to 4-30-2012)

In both Figures 14 and 15, the 0.61 mm nozzle exhibits an upward trend in HTA production rate with an increase in temperature. The 0.84 mm nozzle exhibits an upward trend between 30 and 45°C, however, the point at 20°C does not fit the trend. The 0.84 mm nozzle may produce different results than the 0.61 mm nozzle; or, the difference could be attributed to experimental error. As with determining optimum collapse conditions, further experiments should be conducted to confirm observed trends.

It was initially hypothesized that a smaller nozzle diameter and a lower pool temperature would create ideal collapse conditions, since smaller bubbles immersed in a more extreme temperature would have a more violent collapse. For this set of experiments, part of the initial prediction was correct, as the smaller nozzle did indeed produce the greatest amount of •OH. However, further testing needs to be conducted to ensure reproducibility, rule out experimental error, and draw more concrete conclusions for changing conditions.

CONCLUSIONS

In this study, steam bubble cavitation was explored as a technique to generate •OH. After iterative experimentation and calculation, a temperature-constant reactor was constructed to produce steam bubble cavitation. Steam was injected into the reactor pool-water solution containing terephthalate. Upon the collapse of the steam bubble, •OH was generated and reacted selectively to produce hydroxyterephthalate, a fluorescent product. By varying nozzle diameter and pool-water solution temperature, six conditions were tested to determine the optimum parameters for •OH formation. Results indicated that a nozzle diameter of 0.61 mm and a pool-water solution temperature of 45°C produced the most •OH. Additional experimentation is required to confirm the results and establish any experimental error. Further studies are also necessary to test additional conditions in order to establish trends and determine optimum parameters for •OH formation in steam bubble cavitation.

REFERENCES

[1] Snyder, S. A., Westerhoff, P., Yoon, Y., & Sedlak, D. L. (2003). Pharmaceuticals, Personal Care Products, and Endocrine Disruptors in Water: Implications for the Water Industry. *Environmental Engineering Science, 20* (5), 449-469.

[2] The U.S. Environmental Protection Agency. (2010, October 27). *Pharmaceuticals and Personal Care Products (PPCPs).* Retrieved April 1, 2011 from U.S. EPA: http://www.epa.gov/ppcp/

[3] Naddeo, V., Meric, S., Kassinos, D., Belgiorno, V., & Guida, M. (2009). Fate of pharmaceuticals in contaminated urban wastewater effluent under ultrasonic irradiation. *Water Research, 43*, 4019-4027.

[4] Adewuyi, Y. G. (2005). Sonochemistry in Environmental Remediation. 1. Combinative and Hybrid Sonophotochemical Oxidation Processes for the Treatment of Pollutants in Water. *Environmental Science and Technology, 39* (10), 3409-3420.

[5] Leighton, T. G. (1994). *The Acoustic Bubble.* New York: Academic Press.

[6] Jyoti, K., & Pandit, A. (2001). Water disinfection by acoustic and hydrodynamic cavitation. *Biochemical Engineering Journal, 7*, 201-212.

[7] Mahulkar, A. V., Bapat, P. S., & Pandit, A. B. (2008). Steam Bubble Cavitation. *American Institute of Chemical Engineers Journal, 54* (7), 1711-1724.

[8] Chun, M.-H., Kim, Y.-S., & Park, J.-W. (1996). An investigation of direct condensation of steam jet in subcooled water. *Int. Comm. Heat Mass Transfer, 23* (7), 947-958.

[9] Mason, T., Lorimer, J., Bates, D., & Zhao, Y. (1994). Dosimetry in sonochemistry: the use of aqueous terephthalate ion as a fluorescence monitor. *Ultrasonics Sonochemistry , 1* (2), S91-S95.

[10] Price, G. J., & Lenz, E. J. (1993). The use of dosimeters to measure radical production in aqueous sonochemical systems. *Ultrasonics, 31* (6), 451-456.

[11] Frim, J. A., Rathman, J. F., & Weavers, L. K. (2003). Sonochemical destruction of free and metal-binding ethylenediaminetetraacetic acid. *Water Research, 37*, 3151-3163.

[12] Incropera, F. P., & DeWitt, D. P. (1996). *Fundamentals of Heat and Mass Transfer, Fourth Edition.* New York: John Wiley & Sons.